Journal of Medicinal Chemistry Article

J. Med. Chem. **2010,** *53,* 273–281 **273**
DOI: 10.1021/jm901183d

Discovery of (*Z*)-5-(4-Methoxybenzylidene)thiazolidine-2,4-dione, a Readily Available and Orally Active Glitazone for the Treatment of Concanavalin A-Induced Acute Liver Injury of BALB/c Mice

Youfu Luo,[†,§] Liang Ma,[†,§] Hao Zheng,[†,§] Lijuan Chen,*[,†] Rui Li,[†] Chunmei He,[†] Shengyong Yang,[†] Xia Ye,[†] Zhizhi Chen,[†] Zicheng Li,[‡] Yan Gao,[‡] Jing Han,[†] Gu He,[†] Li Yang,[†] and Yuquan Wei[†]

[†]*State Key Laboratory of Biotherapy, West China Hospital, West China Medical School, Sichuan University, Keyuan Road 4, Gaopeng Street, Chengdu 610041, China and* [‡]*Institute for Chemical Engineering, Sichuan University, Chengdu 610065, China.* [§] *These authors contributed equally.*

Received August 9, 2009

A large amount of evidence suggests that monocytes/macrophages infiltration is implicated in a variety of inflammatory diseases including acute liver injury. Monocyte chemoattractant protein 1 (MCP-1) plays a crucial role in the process of macrophages recruitment. We herein presented a small-molecule library and a feasible quick screening method of evaluating potency of inhibition of chemotaxis of RAW264.7 cells stimulated by MCP-1. Fifty-three small molecules were synthesized and screened, and four compounds (**2g**, **2h**, **4f**, and **6h**) showed inhibitory effects with IC_{50} values range from 0.72 to 20.47 μM, with compound **4f** being the most efficient. Further in vivo studies demonstrated that oral administration of **2g**, **2h**, **4f**, or **6h** decreases, most significantly for **4f**, the serum levels of alanine aminotransaminase (ALT) and asparate aminotransaminase (AST) in ConA-induced acute livery injury BALB/c mice. Histopathological evaluation liver sections confirmed **4f** as a potent, orally active compound for hepatoprotective effects against ConA-induced acute liver injury in BALB/c mice.

Introduction

Acute liver injury, caused by an autoimmune disorder or virus infection, is a severe life-threatening illness. Considerable evidence show that monocytes/macrophages play a crucial role in the process of acute liver injury.[1,2] The activated hepatic macrophages are able to secrete many of components that may interact with hepatocytes and other liver cells. The injured liver renders hepatocytes sensitive to further damage from macrophages products by impairing the ability of hepatocytes to up-regulate normal cellular mechanism of resistance against cytokines secreted by macrophages.[3]

Following liver injury, hepatic stellate cells (HSC) undergo proliferation and migrate into damaged areas in response to chemotactic factors. HSC have been shown to regulate leukocyte trafficking[4] by secreting monocyte chemotactic protein-1 (MCP-1[a]), a major chemotactic factor of the CC subgroup chemokine family, which plays direct role in inflammation and pathogenesis for recruitment and activation of monocytes. Elevated MCP-1 expression has been observed in a large number of tissues during inflammation-dependent disease progression,[5] including atherosclerosis,[6] glomerular nephritides,[7] lung fibrosis,[8] restenosis,[9] arthritis,[10] and cancer.[11] In a mice model of liver injury and human liver disorders, MCP-1 gene expression and serum MCP-1 levels are also markedly elevated.[4,12] In these cases, the influx of macrophages into these tissues stimulated by MCP-1 has been suggested to exacerbate the disease. Thus chemotaxis induced by MCP-1 must be tightly regulated in order to fight for acute liver injury as well as other inflammatory diseases.

Peroxisome proliferator-activated receptor (PPAR)-γ is a member of the nuclear hormone receptor superfamily of ligand-activated transcription factors and is primarily expressed in adipocytes, monocytes, and macrophages. It has shown to inhibit recruitment of macrophages to the sites of inflammation by repressing the transcription of MCP-1 and its receptor CC chemokine receptor 2 (CCR2) in macrophages.[13] Natural and synthetic ligands of PPAR-γ have been shown to inhibit the production of several inflammatory cytokines including IL-1β and TNF-α by macrophages in vitro and inhibit inflammatory reactions in vivo. A recent study demonstrates that the endogenous cyclopentenone prostaglandin 15-deoxy$^{\Delta 12,14}$-prostaglandin J_2, a natural PPAR-γ ligand, reduces the liver injury caused by severe endotoxaemia.[14] Thiazolidinediones (TZDs), which are known to have potent enhancing effects on insulin sensitivity, have been developed for the treatment of noninsulin-dependent diabetes mellitus. It has also been found that TZDs are high-affinity ligands for PPAR-γ and inhibit the production of MCP-1 in some human tissues. Pioglitazone was found to prevent acute liver injury induced by ethanol and lipopolysaccharide.[15] Unfortunately, the first thiazolidinedione, troglitazone, was withdrawn from the market after reports of serious hepatic adverse events. Adverse effects, including congestive heart failure, osteoporosis, weight gain, edema, and anemia, caused by pioglitazone and rosiglitazone, were also reported.[16] It would therefore be highly desirable to find novel therapeutic agents for acute liver injury with fewer adverse effects.

*To whom correspondence should be addressed. Phone: 86-28-85164063. Fax: 86-28-85164060. E-mail: lijuan17@hotmail.com.

[a] Abbreviations: ConA, concanavalin A; MCP-1, monocyte chemoattractant protein 1; TZDs, thiazolidinediones; ALT, aminotransaminase; AST, asparate aminotransaminase; PPAR-γ, peroxisome proliferitor-activated receptor-γ; CCR2, CC chemokine receptor 2.

Published on Web 11/11/2009

Scheme 1. Parallel Synthesis of Barbituric or Thiobarbituric Acid Derivatives[a]

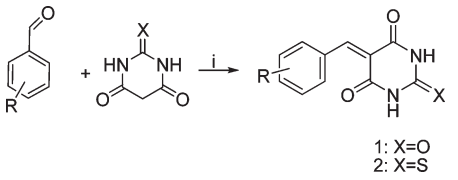

[a] Reagents and conditions: (i) EtOH/H_2O, 80 °C, 3−4 h.

Scheme 2. Parallel Synthesis of 2-Iminothiazolidin-4-one or 2,4-Thiazolidinedione Derivatives [a]

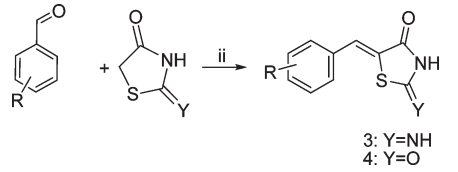

[a] Reagents and conditions: (ii) glacial acetic acid, 1.2 equiv β-alanine, 120 °C, 3 h.

Herein we present a solution-phase parallel synthesis of six structural classes of small molecules and a quick screening method of identifying potential therapeutic agents for acute liver injury, which detects in vitro inhibitory effects on MCP-1 stimulated chemotaxis of macrophage-like RAW264.7 cells. Fifty-three compounds were synthesized through solution parallel synthesis strategy, with four of them (**2g**, **2h**, **4f**, and **6h**) exhibiting high inhibitory effects on the chemotaxis of RAW264.7 with IC_{50} values ranging from 0.72 to 20.47 μM. The most potent one, (*Z*)-5-(4-methoxybenzylidene) thiazolidine-2,4-dione (**4f**), was orally administrated to treat BALB/c mice models of ConA-induced acute liver injury and found capable of decreasing the serum levels of alanine aminotransferase (ALT) and aspartate aminotransferase (AST). Histopathological evaluation of liver sections of **4f**-treated mice further proved that the readily available glitazone **4f** exerts striking hepatoprotective effects against ConA-induced acute liver injury.

Chemistry

To gain quick access to a range of final molecules for biological activity evaluation, a simplified parallel synthesis strategy was developed consisting of a Knoevenagel reaction or Wittig reaction starting from the appropriate aromatic aldehydes. This report describes the synthesis of TZDs and five other new chemical series as potential therapeutic agents for acute liver injury by changing the east part of TZDs (2,4-thiazolidinedione heterocycle), with barbituric acid, thiobarbituric acid, 2-iminothiazolidin-4-one, hydantion, and pyrrolidine-2,5-dione, respectively. Special emphasis was given to the development of a general synthetic method of Knoevenagel reaction that could be applied to these structural classes.

To cover the largest array of chemical reactivity, three distinct Knoevenagel condensation procedures were used as described in procedure A of Scheme 1, using ethanol as solvent, refluxed for 3−4 h, and in procedure B of Scheme 2, using glacial acid as solvent, β-alanine as catalyst, and in procedure C of Scheme 3, using aqueous ethanol as solvents, sodium bicarbonate and ethanolamine as catalyst. The advantages of the procedures were numerous: all starting materials were readily soluble; the reaction was quick and clean; the final insoluble compound was precipitated in the course of the reaction, yielding essentially pure final compound (purities >90%). The phenylmethylene pyrrolidine-2,5-diones were prepared by Wittig reaction using a stable phosphorane intermediate with a benzaldehyde (Scheme 4). At this stage, the products were fully analyzed and characterized before entering the biological tests. The exocyclic double bond is *Z*-configuration in classes of 2,4-thiazolidinediones and 2-iminothiazolidin-4-ones, or *E*-configuration in series of phenylmethylene pyrrolidine-2,5-diones because of the high degree of thermodynamic stability of these isomers[17] because intramolecular hydrogen bond can be formed between the hydrogen atom of in the C−C double bond and the oxygen atom in the heterocyclic part. As to the barbituric or thiobarbituric acids, no *Z* or *E* configuration was involved for the symmetrical structural features.

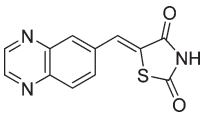

Figure 1. Chemical structure of **7** (AS605240).

Scheme 3. Parallel Synthesis of Phenylmethylenehydantoin Compounds[a]

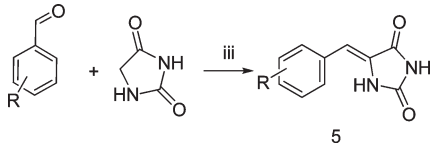

[a] Reagents and conditions: (iii) $NaHCO_3$, aq EtOH, ethanolamine, 120 °C, 5−10 h.

Scheme 4. Parallel Synthesis of Phenylmethylenepyrrolidine-2,5-dione Compounds[a]

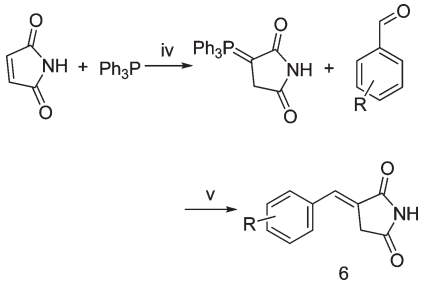

[a] Reagents and conditions: (iv) acetone, reflux, 1 h; (v) methanol, reflux, 1−2 h.

Biological Results and Discussion

Assay for Inhibition of MCP-1-Induced Macrophage-Like RAW264.7 Cells Migration in Vitro. To evaluate the in vitro inhibitory effects of synthetic small molecules on MCP-1-mediated chemotaxis, coincubation of murine macrophage-like cell line RAW264.7 with each of these compounds respectively at an appropriate concentration. AS605240,[18] an established PI3Kγ-specific inhibitor, was proved in our lab to ameliorate ConA-induced acute and chronic liver injury in a murine model.[19] Herein we used **7** (Figure 1) as a positive control compound for in vitro chemotaxis assay. The tested compounds showed different inhibitory effects on

Table 1. Chemotaxis Inhibitory Ratios of the Barbituric Acids or Thiobarbituric Acids Series

compd	R	X	IR[a]@25 μg/mL
7			36.9 ± 2.1
1a	H	O	5.7 ± 3.1
1b	2-OH	O	5.8 ± 1.9
1c	3-OH	O	15.0 ± 3.2
1d	4-OH	O	4.3 ± 2.8
1e	4-Cl	O	4.1 ± 2.0
1f	4-Br	O	5.7 ± 2.1
1g	4-OMe	O	6.2 ± 3.4
1h	4-NMe_2	O	6.2 ± 4.3
1i	3-OMe-4-OH	O	4.1 ± 1.0
1j	3,4-diOMe	O	14.2 ± 4.0
2a	H	S	10.2 ± 1.0
2b	2-OH	S	8.9 ± 1.0
2c	3-OH	S	5.7 ± 3.1
2d	4-OH	S	14.2 ± 2.1
2e	4-Cl	S	4.1 ± 2.0
2f	4-Br	S	4.3 ± 2.8
2g	4-OMe	S	27.4 ± 4.3
2h	4-NMe_2	S	35.7 ± 3.2
2i	3-OMe-4-OH	S	14.4 ± 3.4
2j	3,4-diOMe	S	14.2 ± 4.0

[a] Inhibitory ratios of chemotaxis are defined as follows.

$$\mathrm{IR} = \frac{N_2}{N_1 + N_2} - \mathrm{IR}_0$$

N_1 = the number of migratory cells; N_2 = the number of nonmigratory cells; IR_0 = the inhibitory ratios of chemotaxis without any drug added in the upper chamber. Eight different areas of migrated cells were counted for each well ($n = 3$), the inhibitory ratios were expressed as mean ± SD ($n = 8$, $p < 0.05$).

Table 2. Chemotaxis Inhibitory Ratios of 2-Iminothiazolidin-4-ones and 2,4-Thiazolidinediones Series

compd	R	X	IR[a]@25 μg/mL
7			36.9 ± 2.1
3a	H	NH	10.1 ± 1.0
3b	3-OH	NH	8.7 ± 4.0
3c	4-OH	NH	4.4 ± 3.2
3d	4-Cl	NH	13.0 ± 3.4
3e	4-Br	NH	16.6 ± 1.0
3f	4-OMe	NH	18.6 ± 2.1
3g	4-NMe_2	NH	14.0 ± 2.8
3h	3-OMe-4-OH	NH	19.9 ± 4.3
3i	3,4-diOMe	NH	9.4 ± 2.0
4a	H	O	16.9 ± 4.3
4b	3-OH	O	14.4 ± 3.2
4c	4-OH	O	25.1 ± 3.4
4d	4-Cl	O	12.3 ± 2.2
4e	4-Br	O	16.9 ± 2.8
4f	4-OMe	O	57.8 ± 3.4
4g	4-NMe_2	O	15.8 ± 2.1
4h	3-OMe-4-OH	O	15.8 ± 1.0
4i	3,4-di OMe	O	16.6 ± 4.0

[a] Inhibitory ratios of chemotaxis are defined as follows.

$$\mathrm{IR} = \frac{N_2}{N_1 + N_2} - \mathrm{IR}_0$$

N_1 = the number of migratory cells; N_2 = the number of nonmigratory cells; IR_0 = the inhibitory ratios of chemotaxis without any drug added in the upper chamber. Eight different areas of migrated cells were counted for each well ($n = 3$), the inhibitory ratios were expressed as mean ± SD ($n = 8$, $p < 0.05$).

cells migration at the same concentration (25 μg/mL). The inhibitory ratios of the six chemical series of compounds were illustrated in Tables 1−4.

Table 3. Chemotaxis Inhibitory Ratios of Hydantoins Series

compd	R	IR[a]@25 μg/mL
7		36.9 ± 2.1
5a	3-OH	4.4 ± 3.2
5b	4-OH	13.0 ± 3.4
5c	4-Br	14.0 ± 2.8
5d	4-OMe	19.9 ± 4.3
5e	4-NMe_2	18.6 ± 2.1
5f	3-OMe-4-OH	16.6 ± 1.0
5g	3,4-di OMe	8.7 ± 4.0

[a] Inhibitory ratios of chemotaxis are defined as follows.

$$\mathrm{IR} = \frac{N_2}{N_1 + N_2} - \mathrm{IR}_0$$

N_1 = the number of migratory cells; N_2 = the number of nonmigratory cells; IR_0 = the inhibitory ratios of chemotaxis without any drug added in the upper chamber. Eight different areas of migrated cells were counted for each well ($n = 3$), the inhibitory ratios were expressed as mean ± SD ($n = 8$, $p < 0.05$).

Table 4. Chemotaxis Inhibitory Ratios of Phenylmethylenepyrrolidine-2,5-diones

compd	R	IR[a] @25 μg/mL
7		36.9 ± 2.1
6a	H	5.7 ± 3.1
6b	3-OH	11.4 ± 4.0
6c	4-OH	8.4 ± 3.2
6d	4-Cl	17.9 ± 3.4
6e	4-Br	14.3 ± 1.8
6f	4-OMe	13.3 ± 2.1
6g	4-NMe_2	15.7 ± 2.8
6h	3-OMe-4-OH	39.5 ± 4.3

[a] Inhibitory ratios of chemotaxis are defined as follows.

$$\mathrm{IR} = \frac{N_2}{N_1 + N_2} - \mathrm{IR}_0$$

N_1 = the number of migratory cells; N_2 = the number of nonmigratory cells; IR_0 = the inhibitory ratios of chemotaxis without any drug added in the upper chamber. Eight different areas of migrated cells were counted for each well ($n = 3$), the inhibitory ratios were expressed as mean ± SD ($n = 8$, $p < 0.05$).

Table 5. Chemotaxis IC_{50} Values of Compounds **2g**, **2h**, **4f**, and **6h** on RAW264.7 Cells Migration

	7	**2g**	**2h**	**4f**	**6h**
MW	257	264	277	237	235
IC_{50} (μM)	5.31	11.15	7.20	0.72	20.47

Table 6. Effects of the Potential Therapeutic Agents and **7** on ConA-Induced Liver Injury in Mice ($n = 6$, ave ± SD)

	treatment ALT (U/L)	treatment AST(U/L)
ConA	5734.5 ± 2599.5	4997.9 ± 2619.6
7	1187.5 ± 524.1[b]	1084.5 ± 401.3[a]
2g	3141.2 ± 1469.9[a]	2109.7 ± 844.4[b]
2h	2930.2 ± 1170.8[b]	2072.8 ± 802.6[b]
6h	3304.1 ± 1328.1[a]	3126.9 ± 1358
4f	677.7 ± 375.3[b]	620 ± 199.3[b]

[a] $P < 0.05$. [b] $P < 0.01$ vs controls. Dosages and administration routes: ConA 20 mg/kg intravenously. Potential therapeutic agents 50 mg/kg orally.

It could be seen in Table 1 that the synthesized barbituric acids chemical series exerted low inhibitory potencies against MCP-1 mediated RAW264.7 chemotaxis, while two (**2g** and **2h**) of our synthesized thiobarbituric acids showed comparable effects to that of **7** on chemotaxis. Compound **2g** with

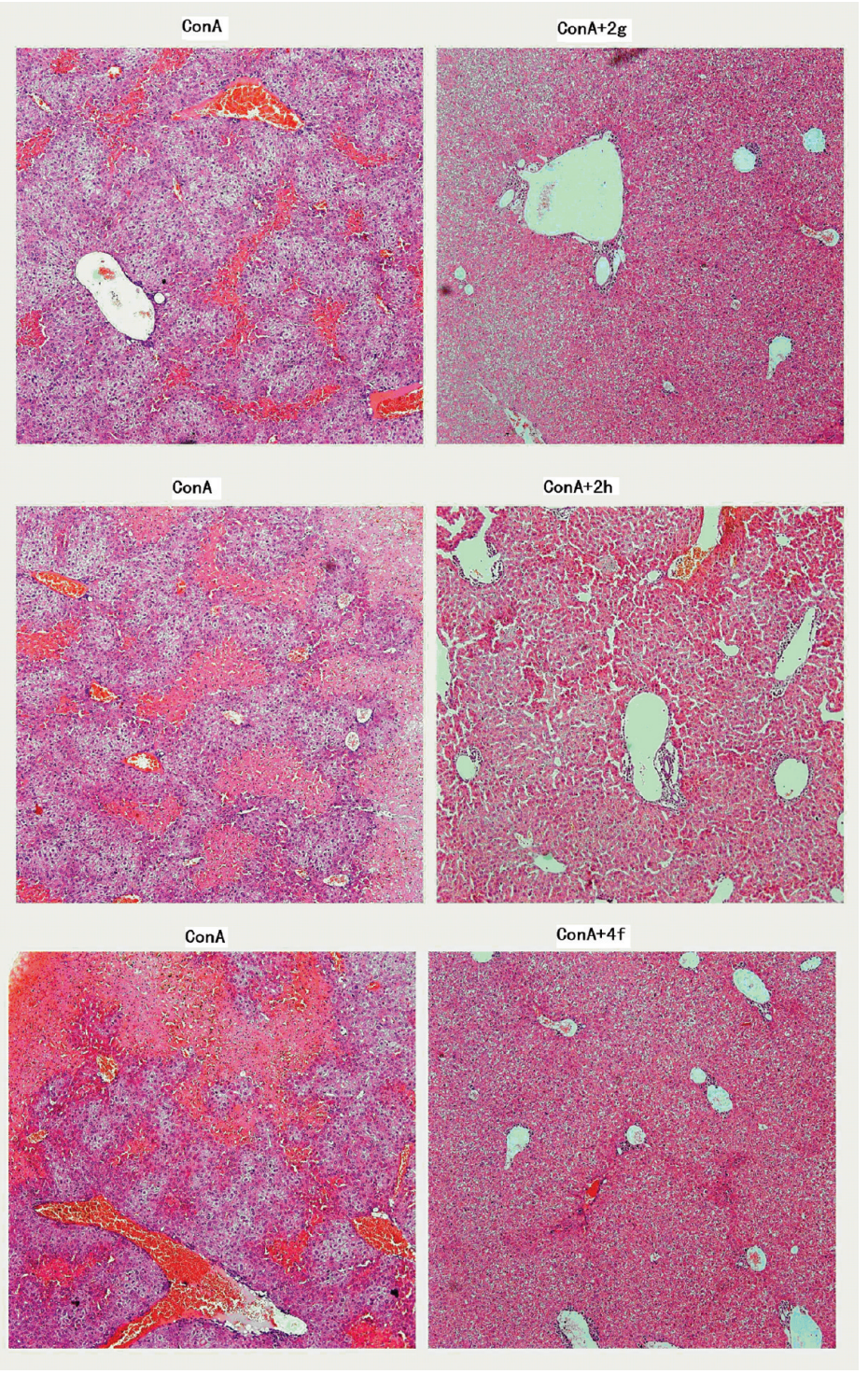

Figure 2. H&E staining of liver sections of untreated and drug-treated acute liver injury mice models challenged ConA.

an inhibitory ratio of 27.4 ± 4.3 has 4-fold higher potency than its counterpart **1g**, with an inhibitory ratio of 6.2 ± 3.4. The potency distinction between **2h** and **1h** is more significant (near to 6-fold). Thus we can make a statement that sulfur atom is superior to oxygen atom in the thiobarbituric acids.

As shown in Table 2, most of the synthesized 2-iminothiazolidin-4-ones analogues showed less potency than that of the corresponding TZDs. (*Z*)-5-(4-Methoxybenzylidene) thiazolidine-2,4-dione (**4f**) is the most potent one among our synthesized TZDs with an inhibitory ratio of 57.8 ± 3.4% against RAW264.7 chemotaxis at concentration of 25 μg/mL. Compound **4f** is quite promising because it is more potent than that of the positive control compound **7** on MCP-1 mediated RAW264.7 chemotaxis, worthy of further biological assays to identify it as a potential agent for acute liver injury.

As shown in Table 3, all the hydantions derivatives exhibit much lower inhibitory ratios against MCP-1 mediated chemotaxis at the given concentration than that of **7**. 5-(4-Hydroxy-3-methoxybenzylidene)pyrrolidine-2,5-dione (**6h**) in Table 4 exerted slightly higher potency than that of **7**.

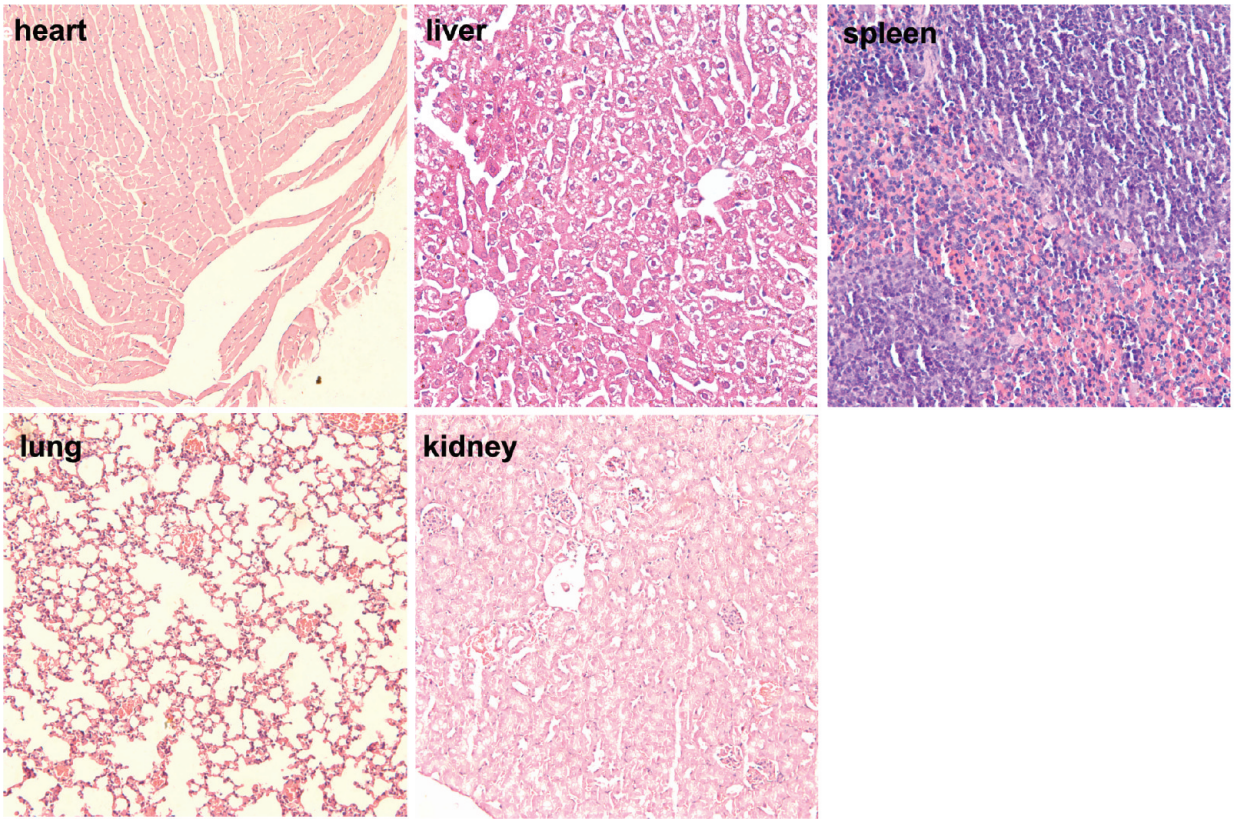

Figure 3. Histomorphological changes of main organs of BALB/c mice 20 h after **4f** treatment. Mice received a single dose of 50 mg/kg **4f** through intragastric administration.

All compounds with the same substituted group on phenyl part in other five chemical series are different from **6h**. Further studies of compounds including **6h** itself in these structural classes are ongoing to clarify the structure−activity relationships.

In conclusion, out of 53 compounds tested in the chemotaxis assay, four compounds in three different structural classes showed sufficient activities for further evaluation and IC_{50} values assay. Two compounds **2g** and **2h** in the chemical series of thiobarbituric acids, one compound **4f** in the class of thiazolidine-2,4-diones and one compound **6h** in the series of pyrrolidine-2,5-diones exerted comparable or higher potencies than **7**. Table 5 showed the IC_{50} values of these four compounds against MCP-1-mediated RAW264.7 cells migration. Compound **4f** showed 7.5-fold decrease compared with **7** with the IC_{50} value at 0.72 μM.

Assay for the Serum Levels of ALT and AST in Treated and Untreated Acute Liver Injury Mice Model. Further in vivo studies in Con A-induced acute hepatitis models confirmed our in vitro finding. After oral administration of our potential therapeutic agents or **7**, the elevated serum levels of AST and ALT were decreased at 20 h after ConA injection to the BALB/c mice. Consistent with our in vitro results, compound **4f** showed protection against Con A-induced liver hepatitis. As shown in Table 6, although **7** showed significant decrease of the serum levels of both ALT and AST, **4f** was the most efficient in decreasing the serum levels among all tested compounds including **7**. These data demonstrated that small molecular inhibitors of chemotaxis of macrophage-like RAW264.7 cells stimulated by MCP-1 play important roles in the protection against inflammatory infiltration to liver tissue in ConA-induced acute hepatitis models.

Histopathological Evaluation. To investigate whether our potential therapeutic agents impaired recruitment of macrophages to liver tissue, liver tissues of drug-treated and control mice were harvested at 4 h after ConA injection for H&E staining assay. As shown in Figure 2, we found the significantly increased number of macrophages in the vessel and sinusoids in liver tissue from ConA injected mice, whereas administration of **2g**, **2h**, or **4f** decreased the necrosis of hepatic cells. The results suggest that these compounds, especially **4f**, modify recruitment of inflammatory cells that is responsible for the development of ConA-induced hepatic injury.

Toxicity Evaluation of Compound 4f. To evaluate the toxicity of **4f**, we conducted H&E staining of main organs of BALB/c mice 20 h after mice receiving a single dose of 50 mg/kg **4f** treatment through intragastric administration. We have not found any tissue pathologic changes of mice after **4f** treatment through H&E staining, including heart, liver, spleen, lung, and kidney (Figure 3). The measurement of transaminase also showed there are no side effects or toxicity on liver (date not show). Pharmacokinetic study was also taken in our group, and the data will be detailed separately in other manuscript. Totally, after oral administration (35 mg/kg), the time to reach the peak concentration was 30 min and the maximal plasma concentration was found to be 4.98 μg/mL. The half time after oral administration was 202.3 min and the oral bioavailability of **4f** was 14.89%.

Conclusion

We described a new compound, glitazone **4f**, and its analogues as potential therapeutic agents for the treatment

of ConA-induce acute liver injury in BALB/c mice model based on a quick in vitro screening method and followed by serum transaminase assay and histophathological evaluation in vivo. Our results indicated that this in vitro screening method for small molecular inhibitors against chemotaxis of macrophage-like RAW264.7 cells stimulated by MCP-1 is an effective approach to find potential therapeutic agents for the treatment of liver hepatitis or other inflammatory diseases. Although **2g** and **2h** in the thiobarbituric acid series were shown to be less potent than that of **7**, glitazone **4f** exhibited the most potent hepatoprotective effects as determined by ALT and AST. Histopathological evaluation further confirmed that this hepatoprotective effect is correlated with a significant decrease in the number of macrophages in the vessel and sinusoids in liver tissue from ConA injected mice.

Experimental Section

Biological Methods. All methods used to evaluate the biological activity of compounds described in this paper have been reported previously.

Cell Culture. RAW264.7 macrophages (American Type Culture Collection, Rockville, MD) were cultured in Dulbecco's modified Eagle's medium (DMEM), 4 mM, L-glutamine, 4.5 g/L glucose supplemented with 10% heat-inactivated fetal bovine serum and 1.5 g/L sodium bicarbonate (7.5% solution) at 37 °C in a humidified atmosphere in the presence of 5% CO_2. Macrophages were subcultured by scraping the cells from the culture medium. RAW264.7 macrophages were used for experiments after reaching passage number 3. The cells were washed once with phosphate buffered saline (D-PBS), removed from the culture dish in DMEM culture medium, and centrifuged at 1000 rpm at room temperature for 3 min. The cell pellet was resuspended in DMEM culture medium and the cell number was determined. Cells (25×10^6) were plated onto one 10 cm culture dish and incubated for 48 h in fresh DMEM culture medium until they reach approximately 80% confluence.

Chemotaxis Assays in Vitro. RAW264.7 cells were starved for 3 h in serum-free medium prior to assaying cells migration. The assays were performed in transwell cell culture chambers with polycarbonate filters (24-well, 8-Millpore), and RAW264.7 cells in 200 μL containing 0.5% BSA and 25 μg/mL of the appropriate drug or DMSO were added to the upper chamber. Then 600 μL of DMEM containing 200 ng/mL MCP-1 (Biovision, USA) was placed in the lower chamber. After maintained for 3 h, the nonmigratory cells ware removed from the upper surface of the filtering membrane by scrapping and washed the filters for 3 times using PBS-buffer, and the cells migrated, in the pore or adhering on the lower membrane were fixed in 4% formalin-PBS buffer for 1 h, stained by the Giemsa staining methods (Nanjing Jiancheng, China). The number of the migrated cells was counted under microscope. The number of migrated cells was taken as the mean of counts in 8 immersion high-power magnitude fields and the standard deviation of the mean value was calculated by 3 repeated chambers.

Animal Models and Treatment. Female BALB/c mice (6−8 weeks old) from Western China Experimental Animal Center were maintained under controlled conditions and had free access to standard laboratory chow and water. All mice received human care according to National Institutes of Health guidelines until they were used for experiment with weight of 20−23 g in the study.

In the acute liver injury studies, mice received an intravenous ConA injection at 15 mg/kg body weight. One of potential therapeutic agents or **7**, suspended in Tween 80 and 5% saline, was administered at a dose of 50 mg/kg by gavage with a 20 gauge animal feeding needle 0.5 h after ConA challenge and control mice received vehicle alone. Serum from cardiac blood was collected 20 h after ConA treatment to determine the levels of ALT and AST. Liver tissue was harvested for histological examination.

Assay for Serum Aminotransferase Levels. Liver injury was quantified by measurement of serum alanine aminotransaminase (ALT) and asparate aminotransaminase (AST) levels using an automated enzyme assay, using a commercial kit and Roche automated analyzers (Roche Diagnostics GmbH, Mannhein, Germany).

Histological Examination. Liver samples were fixed in 4% buffered formalin and embedded in paraffin, and 4 μm sections were stained with hematoxylin and eosin using standard procedure for light microscopic examination to analyze the histological change of tissue structure. Then 10 μm of frozen sections from livers, air-dried, were fixed in cold acetone at 4 °C for 10 min. After washed with PBS, slides were blocked with 10% BSA/PBS for 30 min and then incubated with the primary antibody at 37 °C in a moist, light-protected chamber for 1 h.

Toxicity Evaluation of Compound 4f. To examine the toxicity of **4f**, tissues of heart, lung, spleen, and kidney from normal mice were removed 20 h after **4f** (50 mg/kg, suspended in Tween 80 and 5% saline) was orally administered, and all the tissues were fixed in 10% neutral-buffered formalin, embedded in paraffin, and sections of 3 μm thickness for H&E staining.

Chemistry. Chemical reagents of analytical grade were purchased from Chengdu Changzheng Chemical Factory, Sichuan, PR China. The compounds were synthesized using an EYELA Personal Organic Synthesizer with ChemiStation PPS-CTRL and PPW-20A (Tokyo, Rikakikai) using a 12-well liquid-phase reaction block. TLC was performed on 0.20 mm Silica Gel 60 F_{254} plates (Qingdao Ocean Chemical Factory, Shandong, China). We conformed the purities of all synthetic molecules in present work were ≥95% by HPLC with a phodediode array detector (Waters, Milford, MA) and the chromatographic column was an Atlantis C_{18} (150 mm × 4.6 mm, i.d. 5 μm) (Waters, Milford, Ireland). Nuclear magnetic resonance spectra (NMR) were recorded at 400 MHz on a Varian spectrometer (Varian, Palo Alto, CA) model Gemini 400 and reported in parts per million. Mass spectra (MS) were measured by Q-TOF Priemier mass spectrometer (Micromass, Manchester, UK).

General Procedure for the Synthesis of (Thio)barbituric Acid Derivative Member (1, 2). Aromatic aldehydes (a−j) (3.5 mmol), ethanol (10 mL), distilled water (10 mL), and (thio)barbituric acid (3 mmol) were added in parallel in 12 test tubes with reflux condensers and stirred at 1400 rpm in tubes at 80 °C for 3−4 h. The formed solids were collected by sucking filtration and washed with boiling water (3 × 15 mL), ethanol (3 × 15 mL), and ether (3 × 15 mL). The solids obtained were dried in vacuum for 24 h.

5-Benzylidenepyrimidine-2,4,6(1*H*,3*H*,5*H*)-trione (1a). Yield: 81%, HPLC: 99.2%. ^{1}H NMR (DMSO-d_6, 400 MHz) δ: 7.45−7.56 (m, 3H), 8.08 (d, 2H), 8.27 (s, 1H), 11.24 (s, 1H), 11.40 (s, 1H). MS (ES), m/z: 215.1 (ES−).

5-(2-Hydroxybenzylidene)pyrimidine-2,4,6(1*H*,3*H*,5*H*)-trione (1b). Yield, 80%; HPLC, 98.9%. ^{1}H NMR (DMSO-d_6, 400 MHz) δ: 7.47−8.14 (m, 4H), 8.30 (s, 1H), 11.66 (s, 1H), 12.35 (s, 1H), 12.47 (s, 1H). MS (ES), m/z: 231.0 (ES−).

5-(3-Hydroxybenzylidene)pyrimidine-2,4,6(1*H*,3*H*,5*H*)-trione (1c). Yield, 81%; HPLC, 99.7%. ^{1}H NMR (DMSO-d_6, 400 MHz) δ: 6.95−7.63 (m, 4H), 8.18 (s, 1H), 9.71 (s, 1H), 11.22 (s, 1H), 11.37 (s, 1H). MS (ES), m/z: 231.0 (ES−).

5-(4-Hydroxybenzylidene)pyrimidine-2,4,6(1*H*,3*H*,5*H*)-trione (1d). Yield: 90%, HPLC: 98.8%. ^{1}H NMR (DMSO-d_6, 400 MHz) δ: 6.88 (d, J = 8.8 Hz, 2H), 8.21 (s, 1H), 8.33 (d, J = 8.8 Hz, 2H), 10.80 (s, 1H), 11.13 (s, 1H), 11.26 (s, 1H). MS (ES), m/z: 231.2 (ES−).

5-(4-Chlorobenzylidene)pyrimidine-2,4,6(1*H*,3*H*,5*H*)-trione (1e). Yield, 92%; HPLC, 99.0%. ^{1}H NMR (DMSO-d_6, 400 MHz) δ: 7.54 (d, J = 8.8 Hz, 2H), 8.09 (d, J = 8.8 Hz, 2H), 8.25 (s, 1H), 11.27 (s, 1H), 11.42 (s, 1H). MS (ES), m/z: 249.2 (ES−).

5-(4-Bromobenzylidene)pyrimidine-2,4,6(1*H*,3*H*,5*H*)-trione (1f). Yield, 90%; HPLC, 99.2%. ^{1}H NMR (DMSO-d_6, 400 MHz) δ: 7.68 (d, J = 8.4 Hz, 2H), 7.99 (d, J = 8.4 Hz, 2H), 8.23 (s, 1H), 11.42 (s, 1H), 11.27 (s, 1H). MS (ES) m/z: 293.1 (ES−).

5-(4-Methoxybenzylidene)pyrimidine-2,4,6(1*H*,3*H*,5*H*)-trione (1g). Yield, 95%; HPLC, 98.9%. ^{1}H NMR (DMSO-d_6, 400 MHz) δ: 3.88 (s, 3H), 7.06 (d, J = 8.8 Hz, 2H), 8.25 (s, 1H), 8.37 (d, J = 8.8 Hz, 2H), 11.18 (s, 1H), 11.30 (s, 1H). MS (ES) m/z: 247.5 (ES+), 245.1 (ES−).

5-(4-(Dimethylamino)benzylidene)pyrimidine-2,4,6(1*H*,3*H*,5*H*)-trione (1h). Yield, 93%; HPLC, 98.5%. ^{1}H NMR (DMSO-d_6, 400 MHz) δ: 3.13 (s, 6H), 6.85 (d, J = 8.8 Hz, 2H), 8.15 (s, 1H), 8.43 (d, J = 9.2 Hz, 2H), 10.93 (s, 1H), 11.05 (s, 1H). MS (ES) m/z: 258.2 (ES+), 260.2 (ES−).

5-(4-Hydroxy-3-methoxybenzylidene)pyrimidine-2,4,6(1*H*,3*H*,5*H*)-trione (1i). Yield, 95%; HPLC, 98.4%. ^{1}H NMR (DMSO-d_6, 400 MHz) δ: 3.83 (s, 3H), 6.91 (d, 1H), 7.81 (q, 1H), 8.23 (s, 1H), 8.48 (d, 1H), 10.56 (s, 1H), 11.14 (s, 1H), 11.27 (s, 1H). MS (ES) m/z: 261.2 (ES−).

5-(3,4-Dimethoxybenzylidene)pyrimidine-2,4,6(1*H*,3*H*,5*H*)-trione (1j). Yield, 96%; HPLC, 98.7%. ^{1}H NMR (DMSO-d_6, 400 MHz) δ: 3.81 (s, 3H), 3.89 (s, 3H), 7.12 (d, 1H), 7.91 (d, 1H), 8.26 (s, 1H), 8.41 (s, 1H), 11.19 (s, 1H), 11.31 (s, 1H). MS (ES) m/z: 275.2 (ES−).

5-Benzylidene-2-thioxodihydropyrimidine-4,6(1*H*,5*H*)-dione (2a). Yield, 79%; HPLC, 98.5%. ^{1}H NMR (DMSO-d_6, 400 MHz) δ: 7.02−7.20 (m, 5H), 8.30 (s, 1H), 11.18 (s, 1H), 11.29 (s, 1H). MS (ES) m/z: 230.8 (ES−).

5-(2-Hydroxybenzylidene)-2-thioxodihydropyrimidine-4,6(1*H*,5*H*)-dione (2b). Yield, 80%; HPLC, 99.0%. ^{1}H NMR (DMSO-d_6, 400 MHz) δ: 6.90 (m, 2H), 8.23 (s, 1H), 8.39 (m, 2H), 12.25 (s, 1H), 12.34 (s, 1H). MS (ES) m/z: 247.0 (ES−).

5-(3-Hydroxybenzylidene)-2-thioxodihydropyrimidine-4,6-(1*H*,5*H*)-dione (2c). Yield, 84%; HPLC, 98.5%. ^{1}H NMR (DMSO-d_6, 400 MHz) δ: 6.92−7.71 (m, 4H), 8.19 (s, 1H), 9.92 (s, 1H), 12.33 (s, 1H), 12.44 (s, 1H). MS (ES) m/z: 247.1 (ES−).

5-(4-Hydroxybenzylidene)-2-thioxodihydropyrimidine-4,6-(1*H*,5*H*)-dione (2d). Yield, 87%; HPLC, 98.4%. ^{1}H NMR (DMSO-d_6, 400 MHz) δ: 6.90 (d, J = 8.8 Hz, 2H), 8.24 (s, 1H), 8.39 (d, J = 8.8 Hz, 2H), 10.97 (s, 1H), 12.25 (s, 1H), 12.35 (s, 1H). MS (ES) m/z: 247.0 (ES−).

5-(4-Chlorobenzylidene)-2-thioxodihydropyrimidine-4,6(1*H*,5*H*)-dione (2e). Yield, 93%; HPLC, 99.3%. ^{1}H NMR (DMSO-d_6, 400 MHz) δ: 7.56 (d, J = 8.8 Hz, 2H), 8.14 (d, J = 8.8 Hz, 2H), 8.27 (s, 1H), 12.38 (s, 1H), 12.49 (s, 1H). MS (ES) m/z: 249.2 (ES−).

5-(4-Bromobenzylidene)-2-thioxodihydropyrimidine-4,6(1*H*,5*H*)-dione (2f). Yield, 91%; HPLC, 99.1%. ^{1}H NMR (DMSO-d_6, 400 MHz) δ: 7.69 (d, J = 8.8 Hz, 2H), 8.03 (d, J = 8.8 Hz, 2H), 8.24 (s, 1H), 12.37 (s, 1H), 12.48 (s, 1H). MS (ES) m/z: 308.9 (ES−).

5-(4-Methoxybenzylidene)-2-thioxodihydropyrimidine-4,6-(1*H*,5*H*)-dione (2g). Yield, 90%; HPLC, 99.5%. ^{1}H NMR (DMSO-d_6, 400 MHz) δ: 7.09 (d, J = 8.8 Hz, 2H), 8.27 (s, 1H), 8.43 (d, J = 8.8 Hz, 2H), 12.29 (s, 1H), 12.39 (s, 1H). MS (ES) m/z: 261.3 (ES−).

5-(4-(Dimethylamino)benzylidene)-2-thioxodihydropyrimidine-4,6(1*H*,5*H*)-dione (2h). Yield, 92%; HPLC, 98.4%. ^{1}H NMR (DMSO-d_6, 400 MHz) δ: 3.16 (s, 6H), 6.82 (d, J = 8.8 Hz, 2H), 8.15 (s, 1H), 8.47 (d, J = 8.8 Hz, 2H), 12.04 (s, 1H), 12.14 (s, 1H). MS (ES) m/z: 274.1 (ES−).

5-(4-Hydroxy-3-methoxybenzylidene)-2-thioxodihydropyrimidine-4,6(1*H*,5*H*)-dione (2i). Yield, 98%; HPLC, 98.9%. ^{1}H NMR (DMSO-d_6, 400 MHz) δ: 3.84 (s, 3H), 6.92 (d, 1H), 7.88 (d, 1H), 8.25 (s, 1H), 8.50 (s, 1H), 10.75 (s, 1H), 12.25 (s, 1H), 12.35 (s, 1H). MS (ES) m/z: 277.0 (ES−).

5-(3,4-Dimethoxybenzylidene)-2-thioxodihydropyrimidine-4,6(1*H*,5*H*)-dione (2j). Yield, 93%; HPLC, 98.8%. ^{1}H NMR (DMSO-d_6, 400 MHz) δ: 3.82 (s, 3H), 3.87 (s, 3H), 7.13 (d, 1H), 7.95 (d, 1H), 8.27 (s, 1H), 8.44 (s, 1H), 12.29 (s, 1H), 12.39 (s, 1H). MS (ES) m/z: 291.2 (ES−).

General Procedure for the Synthesis of 2-Iminothiazolidin-4-ones (3, 4). Aromatic aldehydes (3 mmol), 10 mL glacial acetic acid, β-alanine (3.6 mmol), and 2-(imino)thiazolidin-4-one (3 mmol) were mixed in parallel in 12 test tubes with reflux condensers and stirred at 1400 rpm in tubes at 120 °C for 3 h. Then a small portion of water was added and the precipitated solids were collected by sucking filtration and washed with glacial acetic acid (3 × 15 mL) and distilled water (3 × 15 mL). The solids obtained were dried in vacuum at 60 °C for 24 h.

(*Z*)-5-Benzylidene-2-iminothiazolidin-4-one (3a). Yield, 24%; HPLC, 99.6%. ^{1}H NMR (400 MHz, DMSO-d_6) δ: 7.43 (1H, t), 7.50−7.60 (5H, m), 9.19 (1H, s), 9.46 (1H, s). MS (ES): m/z, 203.1 (ES−); m/z, 205.1 (ES+).

(*Z*)-5-(3-Hydroxybenzylidene)-2-iminothiazolidin-4-one (3b). Yield, 35%; HPLC, 99.4%. ^{1}H NMR (400 MHz, DMSO-d_6) δ: 7.50−6.82 (4H, m), 7.53 (1H, m), 9.76 (2H, m), 12.29 (1H, s). MS (ES) m/z, 219.2 (ES−).

(*Z*)-5-(4-Hydroxybenzylidene)-2-iminothiazolidin-4-one (3c). Yield, 63%; HPLC, 97.9%. ^{1}H NMR (400 MHz, DMSO-d_6) δ: 6.76 (2H, m), 7.22 (1H, s), 7.39 (2H, d, J = 8 Hz), 9.25 (2H, s), 9.99 (1H, s). MS (ES): m/z, 219.1 (ES−); m/z, 221.1 (ES+).

(*Z*)-5-(4-Chlorobenzylidene)-2-iminothiazolidin-4-one (3d). Yield, 52%; HPLC, 99.4%. ^{1}H NMR (400 MHz, DMSO-d_6) δ: 6.77 (2H, m), 7.22 (1H, s), 7.39 (2H, d, J = 8 Hz), 9.24 (1H, s), 9.51 (1H, s). MS (ES), m/z: 237.7 (ES−).

(*Z*)-5-(4-Bromobenzylidene)-2-iminothiazolidin-4-one (3e). Yield, 65%; HPLC, 95.4%. ^{1}H NMR (400 MHz, DMSO-d_6) δ: 7.53 (2H, d), 7.58(1H, d), 7.72 (2H, d), 9.23(1H, s), 9.50 (1H, s). MS (ES): m/z, 282.9 (ES−); m/z, 281.0 (ES+).

(*Z*)-5-(4-Methoxybenzylidene)-2-imino-thiazolidin-4-one (3f). Yield, 71%; HPLC, 98.4%. ^{1}H NMR (400 MHz, DMSO-d_6) δ: 3.81 (3H, s), 7.09 (2H, m), 7.51−7.55 (3H, m), 9.15 (2H, br). MS (ES): m/z, 233.1 (ES−); m/z, 235.1 (ES+).

(*Z*)-5-(4-(Dimethylamino)benzylidene)-2-iminothiazolidin-4-one (3g). Yield, 67%; HPLC, 99.1%. ^{1}H NMR (400 MHz, DMSO-d_6) δ: 2.92 (6H, s), 6.68 (2H, d, J = 8 Hz), 7.20 (1H, s), 7.36 (2H, d, J = 8 Hz), 9.05 (1H, s), 9.26 (1H, s). MS (ES): m/z, 246.1 (ES−).

(*Z*)-5-(4-Hydroxy-3-methoxybenzylidene)-2-iminothiazolidin-4-one (3h). Yield, 63%; HPLC, 98.4%. ^{1}H NMR (400 MHz, DMSO-d_6) δ: 3.76 (3H, s), 6.79 (1H, d, J = 8.0 Hz), 7.00 (2H, m), 7.23 (1H, S), 9.09 (1H, s), 9.37 (1H, s). MS (ES): m/z, 249.4 (ES−); m/z, 251.4 (ES+).

(*Z*)-5-(3,4-Dimethoxybenzylidene)-2-iminothiazolidin-4-one (3i). Yield, 65%; HPLC, 97.4%. ^{1}H NMR (400 MHz, DMSO-d_6) δ: 3.82 (6H, s), 7.10−7.16 (3H, m), 7.56 (1H, s), 9.09 (1H, s), 9.37 (1H, s). MS (ES) m/z, 263.3 (ES−).

(*Z*)-5-Benzylidenethiazolidine-2,4-dione (4a). Yield, 84%; HPLC, 99.9%. ^{1}H NMR (DMSO-d_6) δ: 3.47 (t, J = 12 MHz, 1H), 7.39−7.59 (m, 5H), 7.76 (s, 1H). MS (ES) m/z: 204.0 (ES−).

(*Z*)-5-(3-Hydroxybenzylidene)thiazolidine-2,4-dione (4b). Yield, 57%; HPLC, 100%. ^{1}H NMR (DMSO-d_6) δ: 3.49 (d, 1H), 6.98−7.49 (m, 4H), 9.83 (s, 1H). MS (ES) m/z: 220.0 (ES−).

(*Z*)-5-(4-Hydroxybenzylidene)thiazolidine-2,4-dione (4c). Yield, 77%; HPLC, 100%. ^{1}H NMR (DMSO-d_6) δ: 3.49 (d, 1H), 6.92 (d, 2H), 7.44 (d, 2H), 7.70 (s, 1H), 10.30 (s, 1H). MS (ES) m/z: 220.0 (ES−).

(*Z*)-5-(4-Chlorobenzylidene)thiazolidine-2,4-dione (4d). Yield, 85%; HPLC, 98.5%. ^{1}H NMR (DMSO-d_6, 400 MHz) δ: 7.38 (m, 2H), 7.52 (m, 2H), 7.72 (s, 1H), 12.65 (br, 1H). MS (ES) m/z: 237.9 (ES−).

(*Z*)-5-(4-Bromobenzylidene)thiazolidine-2,4-dione (4e). Yield, 85%; HPLC, 98.1%. ^{1}H NMR (DMSO-d_6) δ: 3.45 (t, 1H), 7.61 (q, 2H), 7.77 (m, 2H), 12.67 (s, 1H). MS (ES) m/z: 281.9, 283.9 (ES−).

(*Z*)-5-(4-Methoxybenzylidene)thiazolidine-2,4-dione (4f). Yield, 68%; HPLC, 99.5%. ^{1}H NMR (DMSO-d_6, 400 MHz) δ: 3.82 (s, 3H), 7.09 (m, 2H), 7.55 (m, 2H), 7.77 (s, 1H), 12.56 (br, s, 1H). MS (ES) m/z: 234.0 (ES−).

(*Z*)-5-(4-Dimethylaminobenzylidene)thiazolidine-2,4-dione (4g). Yield, 64%; HPLC, 95.3%. ^{1}H NMR (DMSO-d_6, 400 MHz) δ: 3.09 (s, 6H), 6.76 (d, 2H), 7.45 (d, 2H), 8.05 (s, 1H), 12.4 (s, 1H). MS (ES) m/z: 247.1 (ES−) .

(*Z*)-5-(4-Hydroxy-3-methoxybenzylidene)thiazolidine-2,4-dione (4h). Yield, 95%; HPLC, 97.5%. ^{1}H NMR (DMSO-d_6) δ: 3.80 (s, 3H), 3.49 (d, 1H), 6.92 (d, 1H), 7.07 (q, 1H), 7.17 (d, 1H), 7.72 (s, 1H), 9.95 (s, 1H). MS (ES) m/z: 250.0 (ES−).

(*Z*)-5-(3,4-Dimethoxybenzylidene)thiazolidine-2,4-dione(4i). Yield, 79%; HPLC, 97.4%. ^{1}H NMR (DMSO-d_6, 400 MHz) δ: 3.81 (s, 6H), 6.94−7.22 (m, 3H), 7.95 (s, 2H), 12.6 (s, 1H). MS (ES) m/z: 264.1 (ES−) .

General Procedure for the Synthesis of Phenylmethylenehydantoins (5). Hydantion (1.0 g, 10.0 mmol) was dissolved in 10 mL of water with stirring. After complete dissolution, the pH of the mixture was buffered to 7.0 with saturated $NaHCO_3$ solution. Ethanolamine (0.9 mL) was added to the reaction mixture, and the temperature was increased to 90 °C gradually. The appropriate aldehyde (10.0 mmol) solution in 10 mL of ethanol was added dropwise with continuous stirring. The temperature was raised to 120 °C and kept under reflux at the temperature for 5−10 h depending on the nature of the aldehyde used. The end point of the reaction was determined by TLC. After adequately cooling of the reaction mixture, the precipitated solids was filtered, washed with ethanol/water (1:5, v/v), and recrystallized from ethanol to afford the title product.

(*Z*)-5-(3-Hydroxybenzylidene)imidazolidine-2,4-dione (5a). Yield, 33%; HPLC, 99.7%. ^{1}H NMR (DMSO-d_6, 400 MHz) δ: 6.31 (s, 1H), 6.73−7.22 (m, 4H), 9.51 (s, 1H), 10.48 (s, 1H), 11.19 (s, 1H). MS (ES) m/z: 203.1 (ES−).

(*Z*)-5-(4-Hydroxybenzylidene)imidazolidine-2,4-dione (5b). Yield, 51%; HPLC, 98.6%. ^{1}H NMR (DMSO-d_6, 400 MHz) δ: 6.35 (s, 1H), 6.79 (d, 2H), 7.46 (d, 2H), 9.86 (s, 1H), 10.33 (s, 1H), 11.12 (s, 1H). MS (ES) m/z: 203.0 (ES−).

(*Z*)-5-(4-Bromobenzylidene)imidazolidine-2,4-dione (5c). Yield, 80%; HPLC, 99.6%. ^{1}H NMR (DMSO-d_6, 400 MHz) δ: 5.18 (s, 1H), 7.35−7.85 (m, 4H), 9.24 (s, 1H), 10.0 (s, 1H). MS (ES) m/z: 265.0, 267.0 (ES−).

(*Z*)-5-(4-Methoxybenzylidene)imidazolidine-2,4-dione (5d). Yield, 23%; HPLC, 99.3%. ^{1}H NMR (DMSO-d_6, 400 MHz) δ: 3.80 (s, 3H), 6.39 (s, 1H), 6.95 (d, 2H), 7.58 (d, 2H), 10.44 (s, 1H), 11.17 (s, 1H). MS (ES) m/z: 217.1 (ES−).

(*Z*)-5-(4-Dimethylaminobenzylidene)imidazolidine-2,4-dione (5e). Yield, 75%; HPLC, 95.7%. ^{1}H NMR (DMSO-d_6, 400 MHz) δ: 3.12 (s, 6H), 6.31 (s, 1H), 6.71 (d, 2H), 7.15 (d, 2H), 10.43 (s, 1H), 11.16 (s, 1H). MS (ES) m/z: 230.1 (ES−).

(*Z*)-5-(4-Hydroxy-3-methoxybenzylidene)imidazolidine-2,4-dione (5f). Yield, 14%; HPLC, 98.5%. ^{1}H NMR (DMSO-d_6, 400 MHz) δ: 3.84 (s, 3H), 6.36 (s, 1H), 6.80−7.12 (m, 3H), 9.43 (s, 1H), 10.42 (s, 1H), 11.13 (s, 1H). MS (ES) m/z: 233.1 (ES−).

(*Z*)-5-(3,4-Dimethoxybenzylidene)imidazolidine-2,4-dione (5g). Yield, 24%; HPLC, 95.6%. ^{1}H NMR (DMSO-d_6, 400 MHz) δ: 3.83 (s, 6H), 6.31 (s, 1H), 6.94−7.15 (m, 3H), 10.40 (s, 1H), 11.30 (s, 1H). MS (ES) m/z: 247.0 (ES−).

General Procedure for the Synthesis of Pyrrolidine-2,5-diones (6). Aromatic aldehydes (3 mmol), anhydrous methanol (10 mL), and triphenylphosphoranylidene succinimide (3 mmol) were added in parallel in 12 test tubes with reflux condensers and stirred at 1400 rpm in tubes at reflux temperature for 1.5 h. The formed precipitates were collected by sucking filtration and washed with methanol (3 × 15 mL). The solids obtained were dried in vacuum at room temperature for 24 h.

(*E*)-3-Benzylidenepyrrolidine-2,5-dione (6a). Yield, 35%; HPLC, 98.4%. ^{1}H NMR (400 MHz, DMSO-d_6) δ: 3.65 (2H, d), 7.38−7.63 (6H, m), 11.45 (1H, s). MS (ES) m/z: 186.0 (ES−).

(*E*)-3-(3-Hydroxybenzylidene)pyrrolidine-2,5-dione (6b). Yield, 95%; HPLC, 98.4%. ^{1}H NMR (400 MHz, DMSO-d_6) δ: 3.52 (2H, d), 5.22−6.75 (5H, m), 9.56 (1H, s), 11.36 (1H, s). MS (ES) m/z: 202.1 (ES−).

(*E*)-3-(4-Hydroxybenzylidene)pyrrolidine-2,5-dione (6c). Yield, 72%; HPLC, 99.4%. ^{1}H NMR (400 MHz, DMSO-d_6) δ: 3.50 (2H, d), 6.77−6.87 (2H, m), 7.22 (1H, s), 7.39 (2H, d), 9.99 (1H, s), 11.23 (1H, s). MS (ES), m/z: 202.1 (ES−).

(*E*)-3-(4-Chlorobenzylidene)pyrrolidine-2,5-dione (6d). Yield, 87%; HPLC, 95.4%. ^{1}H NMR (400 MHz, DMSO-d_6) δ: 3.57 (2H, d), 7.31 (1H, t), 7.46 (2H, d), 7.58 (2H, d), 11.40 (1H, s). MS (ES), m/z: 220.0 (ES−).

(*E*)-3-(4-Bromobenzylidene)pyrrolidine-2,5-dione (6e). Yield, 90%; HPLC, 96.4%. ^{1}H NMR (400 MHz, DMSO-d_6) δ: 3.63 (2H, d), 7.36 (1H, d), 7.58 (2H, d), 7.66 (2H, d), 11.48 (1H, s). MS (ES) m/z: 264.0 (100.0%), 266.0 (ES−).

(*E*)-3-(4-Methoxybenzylidene)pyrrolidine-2,5-dione (6f). Yield, 84%; HPLC, 99.0%. ^{1}H NMR (400 MHz, DMSO-d_6) δ: 3.52 (2H, d), 3.74 (3H, s), 6.95 (2H, d), 7.27 (1H, s), 7.51 (2H, d), 11.28 (1H, s). MS (ES) m/z: 216.0 (ES−).

(*E*)-3-(4-(Dimethylamino)benzylidene)pyrrolidine-2,5-dione (6g). Yield, 91%; HPLC, 99.3%. ^{1}H NMR (400 Hz, DMSO-d_6) δ: 2.92 (6H, s), 3.48 (2H, d), 6.69 (2H, d), 7.20 (1H, s), 7.37 (2H, d), 7.53 (1H, s). MS (ES) m/z: 229.1 (ES−).

(*E*)-3-(4-Hydroxy-3-methoxybenzylidene)pyrrolidine-2,5-dione (6h). Yield, 87%; HPLC, 99.4%. ^{1}H NMR (400 MHz, DMSO-d_6) δ: 3.57 (2H, d), 3.74 (3H, s), 6.78−7.08 (2H, m), 7.23 (1H, s), 9.60 (1H, s). MS (ES) m/z: 232.1 (ES−).

Acknowledgment. We are grateful to the National Major Program of China during the 11th Five-Year Plan Period (2009ZX09102-045) and the National Science Foundation of China (30901743).

References

(1) Holt, M. P.; Cheng, L.; Ju, C. Identification and characterization of infiltrating macrophages in acetaminophen-induced liver injury. *J. Leukocyte Biol.* **2008**, *84*, 1410–1421.
(2) Duffield, J. S.; Forbes, S. J.; Constandinou, C. M.; Clay, S.; Partolina, M.; Vuthoori, S.; Wu, S.; Lang, R.; Iredale, J. P. Selective depletion of macrophages reveals distinct, opposing roles during liver injury and repair. *J. Clin. Invest.* **2005**, *115*, 56–65.
(3) Czaja, M. J.; Geerts, A.; Xu, J.; Schmiedeberg, P.; Ju, Y. Monocyte chemoattractant protein 1 (MCP-1) expression occurs in toxic rat liver injury and human liver disease. *J. Leukocte Biol.* **1994**, *55*, 120–126.
(4) Marra, F.; Romanelli, R. G.; Giannini, C.; Failli, P.; Pastacaldi, S.; Arrighi, M. C.; Pinzani, M.; Laffi, G.; Montalto, P.; Gentilini, P. Monocyte Chemotactic Protein-1 as a Chemoattractant for Human Hepatic Stellate Cells. *Hepatology* **1999**, *29*, 140–148.
(5) Melgarejo, E.; Medina, M. A.; Sánchez-Jiménez, F.; Urdiales, J. L. Monocyte chemoattractant protein-1: a key mediator in inflammatory processes. *Int. J. Biochem. Cell Biol.* **2009**, *41*, 998–1001.
(6) Shin, W. S.; Szuba, A.; Rockson, S. G. The role of chemokines in human cardiovascular pathology: enhanced biological insights. *Atherosclerosis* **2002**, *160*, 91–102.
(7) Grandaliano, G.; Gesualdo, L.; Ranieri, E.; Monno, R.; Montinaro, V.; Marra, F.; Schena, F. P. Monocyte chemotactic peptide-1 expression in acute and chronic human nephritides: a pathogenetic role in interstitial monocytes recruitment. *J. Am. Soc. Nephrol.* **1996**, *7*, 906–913.
(8) Zhang, K.; Phan, S. H. Cytokines and pulmonary fibrosis. *Biol. Signals* **1996**, *5*, 232–239.
(9) Usui, M.; Egashira, K.; Ohtani, K.; Kataoka, C.; Ishibashi, M.; Hiasa, K.-I.; Katoh, M.; Kitamoto, S.; Takeshita, A. Anti-monocyte chemoattractant protein-1 gene therapy inhibits restenotic changes (neointimal hyperplasia) after balloon injury in rats and monkeys. *FASEB J.* **2002**, *16*, 1838–1840.
(10) Taylor, P. C.; Peters, A. M.; Paleolog, E.; Chapman, P. T.; Elliott, M. J.; McCloskey, R.; et al. Reduction of chemokine levels and leukocyte traffic to joints by tumor necrosis factor alpha blockade in patients with rheumatoid arthritis. *Arthrit. Rheum.* **2000**, *43*, 38–47.
(11) O'Hayre, M.; Salanga, C. L.; Handel, T. M.; Allen, S. J. Chemokines and cancer: migration, intracellular signalling and intercellular communication in the microenvironment. *Biochem. J.* **2008**, *409*, 635–49.
(12) Van Coillie, E.; Van Damme, J.; Opdenakker, G. The MCP/eotaxin subfamily of CC chemokines. *Cytokine Growth Factor Rev.* **1999**, *10*, 61–86.

(13) Yatrik, M.; Shah, K. M.; Frank, J. G. Expression of peroxisome proliferator-activated receptor-γ in macrophage suppresses experimentally induced colitis. *Am. J. Physiol., Gastrointest. Liver Physiol.* **2007**, *292*, G657–G666.
(14) Collin, M.; Thiemermann, C. The PPAR-γ ligand 15-deoxy$^{\Delta 12,14}$ prostaglandin J_2 reduces the liver injury in endotoxic shock. *Eur. J. Pharmacol.* **2003**, *29*, 257–258.
(15) Ohata, M.; Suzuki, H.; Sakamoto, K; Hashimoto, K; Nakajima, H; Yamauchi, M; Hokkyo, K; Yamada, H; Toda, G. Pioglitazone Prevents Acute Liver Injury Induced by Ethanol and Lipopolysaccharide Through the Suppression of Tumor Necrosis Factor-(alpha). *Alcohol: Clin. Exp. Res.* **2004**, *28*, 139S–144S.
(16) Yki-Jarvinen, H. Drug Therapy—Thiazolidinediones. *N. Engl. J. Med.* **2004**, *351*, 1106–1118.
(17) Xu, Z.; Knaak, C.; Ma, J.; Beharry, Z. M.; McInnes, C.; Wang, W.; Kraft, A. S.; Smith, C. D. Synthesis and Evaluation of Novel Inhibitors of Pim-1 and Pim-2 Protein Kinases. *J. Med. Chem.* **2009**, *52*, 74–86.
(18) Camps, M.; Ruckle, T.; Ji, H.; Ardissone, V.; Rintelen, F.; Shaw, J.; Ferrandi, C.; Chabert, C.; Gillieron, C.; Francon, B.; Martin, T.; Gretener, D.; Perrin, D.; Leroy, D.; Vitte, P.-A.; Hirsch, E.; Wymann, M. P.; Cirillo, R.; Schwarz, M. K.; Rommel, C. Blockade of PI3kg suppresses joint inflammation and damage in mouse models of rheumatoid arthritis. *Nature Med.* **2005**, *11*, 936–941.
(19) Wang, Z.; Wu, X.; Song, L.; Wang, Y.; Hu, X.; Luo, Y.; Chen, Z.; Ke, J.; Peng, X.; He, C.; Zhang, W.; Chen, L.; Wei, Y. Phosphoinositide 3-kinase γ inhibitor ameliorates concanavalin A-induced hepatic injury in mice. *Biochem. Biophys. Res. Commun.* **2009**, *386*, 569–574.